Available online at www.sciencedirect.com
ScienceDirect
Renewable Energy 32 (2007) 547–566
RENEWABLE ENERGY
www.elsevier.com/locate/renene

Performance of low-temperature differential Stirling engines

Bancha Kongtragool, Somchai Wongwises*

Fluid Mechanics, Thermal Engineering and Multiphase Flow Research Lab. (FUTURE), Department of Mechanical Engineering, King Mongkut's University of Technology Thonburi, Bangmod, Bangkok 10140, Thailand

Received 1 March 2006; accepted 2 March 2006
Available online 18 April 2006

Abstract

In this paper, two single-acting, twin power piston and four power pistons, gamma-configuration, low-temperature differential Stirling engine are designed and constructed. The engine performance is tested with air at atmospheric pressure by using a gas burner as a heat source. The engine is tested with various heat inputs. Variations of engine torque, shaft power and brake thermal efficiency at various heat inputs with engine speed and engine performance are presented. The Beale number obtained from testing of the engines is also investigated. The results indicate that, for twin power piston engine, at a maximum actual heat input of 2355 J/s with a heater temperature of 589 K, the engine produces a maximum torque of 1.222 N m at 67.7 rpm, a maximum shaft power of 11.8 W at 133 rpm, and a maximum brake thermal efficiency of 0.494% at 133 rpm, approximately. For the four power pistons engine, the results indicate that at the maximum actual heat input of 4041 J/s with the heater temperature of 771 K, the engine produces a maximum torque of 10.55 N m at 28.5 rpm, a maximum shaft power of 32.7 W at 42.1 rpm, and a maximum brake thermal efficiency of 0.809% at 42.1 rpm, approximately.

Keywords: Stirling engine; Hot-air engine; Regenerative heat engine

1. Introduction

The Stirling engine is a simple type of external-combustion engine. The Stirling engine was the first invented regenerative cycle heat engine. Robert Stirling patented the Stirling

*Corresponding author. Tel.: +662 4709115; fax: +662 4709111.
E-mail address: somchai.won@kmutt.ac.th (S. Wongwises).

0960-1481/$ - see front matter © 2006 Elsevier Ltd. All rights reserved.
doi:10.1016/j.renene.2006.03.003

Nomenclature

C_P	specific heat of water at constant pressure (4186 J/kg K)
E_H	heat source efficiency
E_{BT}	brake thermal efficiency
f	engine frequency (Hz)
H	lower heating value of the gas used (46 MJ/kg)
m_f	mass of gas burned (kg)
m_w	mass of water to absorb heat (kg)
N	engine speed (rpm, rps)
N_B	Beale number (W/bar cc Hz)
P	shaft power (W)
p_m	engine mean pressure (bar)
q_{in}	actual heat input to the engine (J/s)
q_S	total heat input from heat source (J/s)
r	dynamometer brake drum radius (m)
S	spring balance reading (N)
T	engine torque (N m)
T_C	cooler temperature (K)
T_H	heater temperature (K)
T_{w1}	initial water temperature (K)
T_{w2}	maximum water temperature after the heat source has been turned off (K)
V_P	power-piston swept volume (cc)
W	loading weight (N)

Greek letter

τ	cooler to heater temperature ratio

engine in 1816 (patent no. 4081) [1]. Engines based upon his invention were built in many forms and sizes until the turn of the century. Because Stirling engines were simple and safe to operate, ran almost silently on any combustible fuel, and were clean and efficient compared to steam engines, they were quite popular [2]. These Stirling engines were small and the power produced from the engine was low (100 W to 4 kW). The first era of the Stirling engine was terminated by the rapid development of the internal-combustion engine and the electric motor.

The second era of the Stirling engine began around 1937 [2], when the Stirling engine was brought to a high state of technological development by the Philips Research Laboratory in Eindhoven, Holland, and has progressed continuously since that time. Initial work focused on the development of small thermal-power electric generators for radios and similar equipment used in remote areas [2,3].

New materials were one of the keys to the Stirling engine success; the Philips research team used new materials, such as stainless steel [2]. Another key to success was having a better knowledge of thermal and fluid physics than in the first era. The specific power of

the small "102C" engine of 1952 was 30 times that of the old Stirling engines [4]. The progress in further development by Philips and many industrial laboratories, together with the need for more energy resources, has sustained the second era of Stirling engine development until today [2].

The low temperature differential (LTD) Stirling engine is a type of Stirling engine that can operate with a low-temperature heat source. There are many low-temperature heat sources available including solar energy. The LTD Stirling engine then provides the possibility of direct conversion of solar energy to mechanical work.

A LTD Stirling engine can be run with a small temperature difference between the hot and cold ends of the displacer cylinder [1]. LTD Stirling engines provide value as demonstration units, but they immediately become of interest when considering the possibility of power generation from many low-temperature waste heat sources in which the temperature is less than 100 °C [5]. Some characteristics of the LTD Stirling engine are as follow [1]:

(1) Displacer to power piston swept volumes ratio or compression ratio is large.
(2) Diameters of displacer cylinder and displacer are large.
(3) Displacer length is short.
(4) Effective heat transfer surfaces on both end plates of the displacer cylinder are large.
(5) Displacer stroke is small.
(6) Dwell period at the end of the displacer stroke is rather longer than the normal Stirling engine.
(7) Operating speed is low.

Many works on common Stirling engines, LTD Stirling engines and solar-powered Stirling engines have been investigated in the authors' former work [6]. Among many researches, some works related to the LTD Stirling engine are as follows [6]:

In 1975, Haneman [7] studied the possibility of using air with low temperature sources. An unusual engine, in which the exhaust heat was still sufficiently hot to be useful for other purposes, was constructed. This kind of engine was reported by Spencer [8] in 1989 that, in practice, it would produce little useful work relative to the collector system size, and would give little gain compared to the additional maintenance required.

A simply constructed low temperature heat engine modeled on the Stirling engine configurations was patented in 1983 by White [9]. White [9] suggested improving the performance by pressurizing the displacer chamber. Efficiencies were claimed to be around 30%, but this can be regarded as quiet high for a low-temperature engine.

In 1984, O'Hare [10] patented a device passing cooled and heated streams of air through a heat exchanger for changing the pressure of air inside the bellows. The practical usefulness of this device was not shown in detail as was in the case of Haneman's work.

Kolin [1,2] experimented with a number of LTD Stirling engines, over a period of many years. In 1983, he presented a model that worked on a temperature difference between the hot and cold ends of the displacer cylinder as low as 15 °C.

After Kolin published his work, Senft [5] made an in-depth study of the Ringbom engine and its derivatives, including the LTD engine. Senft's research in LTD Stirling engines resulted in a most interesting engine, which had an ultra-low temperature difference of 0.5 °C. It was very difficult to create any development better than this result. Senft's work

in 1991 [11], showing the principal motivation for using Stirling and general heat engines, developed an engine operating with a temperature difference of 2 °C or lower.

In 1993, Senft [2] described the design and testing of a small LTD Ringbom Stirling engine powered by a 60° conical reflector. He reported that the tested 60° conical reflector, producing hot end temperature of 93 °C under running conditions, worked very well.

In 1997, Iwamoto et al. [12] compared the performance of a LTD Stirling engine with a high-temperature differential Stirling engine. Finally, they concluded that the LTD Stirling engine efficiency at its rated speed was approximately 50% of the Carnot efficiency. However, the compression ratio of their LTD Stirling engine was approximately equal to that of a conventional Stirling engine. Then, its performance seemed to be the performance of a common Stirling engine operating at a low temperature.

In 2003, Kongtragool and Wongwises [13] made a theoretical investigation on the Beale number for LTD Stirling engines. The existing Beale number data for various engine specifications were collected from literatures. They concluded that the Beale number for a LTD Stirling engine could be found from the mean-pressure power formula.

In 2005, Kongtragool and Wongwises [14] investigated, theoretically, the power output of the gamma-configuration LTD Stirling engine. The former works on Stirling-engine power output calculation were studied and discussed. They pointed out that the mean-pressure power formula was the most appropriate for LTD Stirling-engine power output estimation. However, the hot-space and cold-space working fluid temperature was needed in the mean-pressure power formula.

In 2005, Kongtragool and Wongwises [15] presented the optimum absorber temperature of a once-reflecting full-conical reflector for a LTD Stirling engine. A mathematical model for the overall efficiency of a solar-powered Stirling engine was developed. Both limiting conditions of maximum possible engine efficiency and power output were studied. Results showed that the optimum absorber temperatures obtained from both conditions were not significantly different and the overall efficiency in the case of the maximum possible engine power output was very close to that of the real engine of 55% Carnot efficiency.

As described above, there is only one published paper on the experimental results of the LTD Stirling engine [2]. However, this engine is a Ringbom Stirling engine. No paper has been published on the experimental results of the kinematic LTD Stirling engine.

In this article, the design, construction and testing of two kinematic single-acting, twin power piston and four power pistons, gamma-configuration, LTD Stirling engine are presented. Non-pressurized air is used as working fluid. The heat source used is a domestic gas burner.

2. Engine design and construction

The schematic diagrams of the test engines are shown in Figs. 1 and 2. Main engine design parameters are shown in Tables 1 and 2. They are designed in single-acting, gamma-configuration. Since the gamma-configuration provides a large regenerator heat transfer area [12] and is easy to be constructed [1], this configuration is used in the present study. The power cylinders are directly connected to the cooler plate to minimize the cold-space and transfer-port dead volume. The cooling water pan is a part of the cooler plate.

In order to make the engine compact and minimize the number of engine parts, a simple crank mechanism is used in this engine. The crankshaft is made from a steel shaft, two crank discs and a crank pin. The crank pin is connected to the displacer connecting rod.

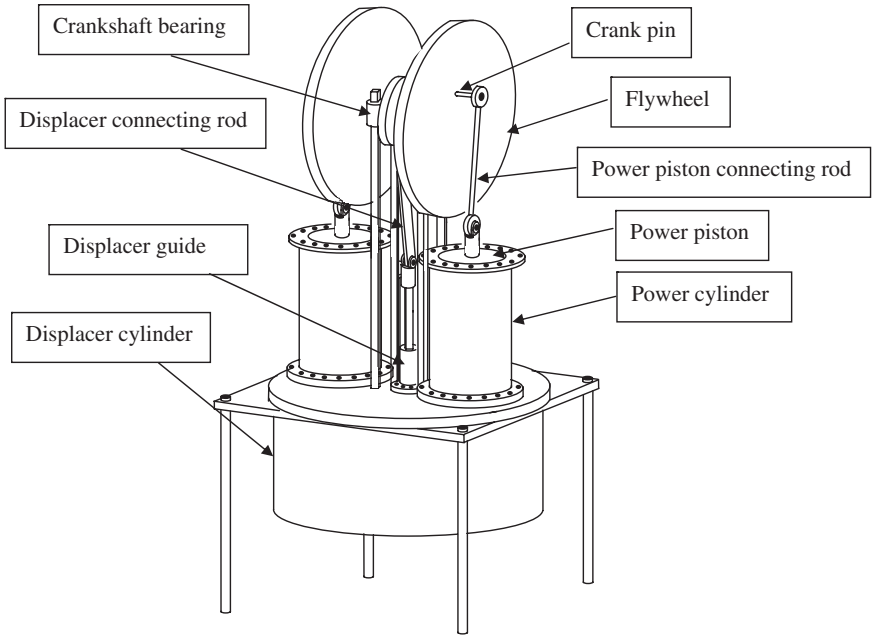

Fig. 1. Schematic diagram of the twin power piston Stirling engine.

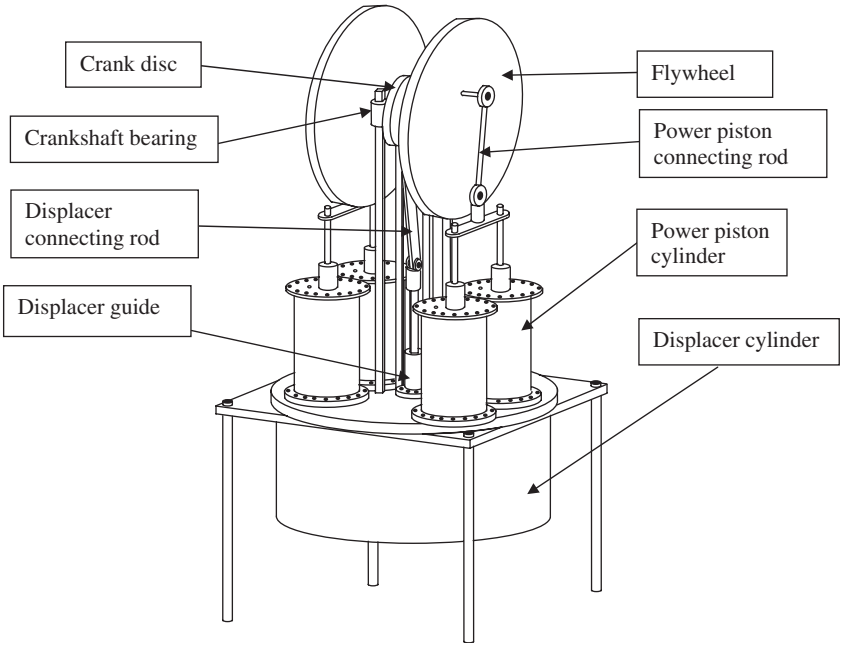

Fig. 2. Schematic diagram of the four power pistons Stirling engine.

Table 1
Main design parameters of twin power piston engine

Mechanical configuration	Gamma
Power piston:	
Bore × stroke (cm)	8.3 × 8.26
Swept volume (cc)	893.8
Displacer:	
Bore × stroke (cm)	32 × 7.95
Swept volume (cc)	6393.8
Compression ratio	7.15
Phase angle	90°

Table 2
Main design parameters of four power pistons engine

Mechanical configuration	Gamma
Power piston:	
Bore × stroke (cm)	13.3 × 13.3
Swept volume (cc)	7391
Displacer:	
Bore × stroke (cm)	60 × 14.48
Swept volume (cc)	40 941
Compression ratio	5.54
Phase angle	90°

The crankshaft is supported by two ball bearings. Two steel flywheels are attached to both ends of the crankshaft. These flywheels also act as the crank discs for the power piston.

The power cylinders are made from a steel pipe. The cylinder bores are finished by turning. The power pistons are made from a steel pipe and plate. The power piston cylindrical surfaces are brass lined and then turned to match the power cylinder bores. The clearance between the piston and bore is 0.02 mm, approximately. The oil grooves, 1 mm × 1 mm with 10 mm spacing are provided on the cylindrical piston surfaces.

For the twin power piston engine, the displacer cylinder and head are made from a 0.5 mm thick stainless steel Indian pan. The displacer swept volume is 6394 cc with 32 cm bore and 7.95 cm stroke. The power piston bore and stroke is 8.3 and 8.26 cm, respectively. The compression ratio of this engine is 7.15.

For the four power pistons engine, the displacer cylinder and head is made from a 1 mm thick stainless steel plate. The displacer swept volume is 40 941 cc with 60 cm bore and 14.48 cm stroke. The power piston bore and stroke is 13.3 and 13.3 cm, respectively. The compression ratio of this engine is 5.54.

The displacer of this engine serves as a regenerator. This moving regenerator is made from a perforated steel sheet with a round-hole pattern. A stainless steel pot scourer is used as the regenerator matrix. The clearance between the displacer and its cylinder of the twin power piston and the four power piston engines are 1 and 2 mm, approximately.

A stainless steel pipe is used as a displacer rod. The displacer rod is guided by two brass bushings placed in the displacer rod guide housing. Two rubber seals are used to prevent leakage through the displacer rod guide bushings.

The power piston and displacer connecting rod is made from a steel rod. Both ends of the connecting rod are attached to two ball bearing housings.

3. Experimental apparatus

The engine and testing facilities are shown in Fig. 3. Details of other experimental apparatus are as follows:

Since the engine speed is low, a rope-brake dynamometer can be used to measure the engine torque. The brake drum diameters of the twin power piston and the four power pistons engine are 29.3 and 17.9 cm, respectively. The braking load is measured by the loading weight and the spring balance reading. A photo tachometer with ± 0.1 rpm accuracy is used to measure the engine speed.

The cooling water is supplied from a cooling water system. The cooler temperature, T_C, is measured by three T-type thermocouples. The heater temperature, T_H, is measured by three K-type thermocouples. A data logger and a personal computer are used to collect data from the thermocouples. The accuracy of the temperature measurement is $\pm 0.001\,^{\circ}C$.

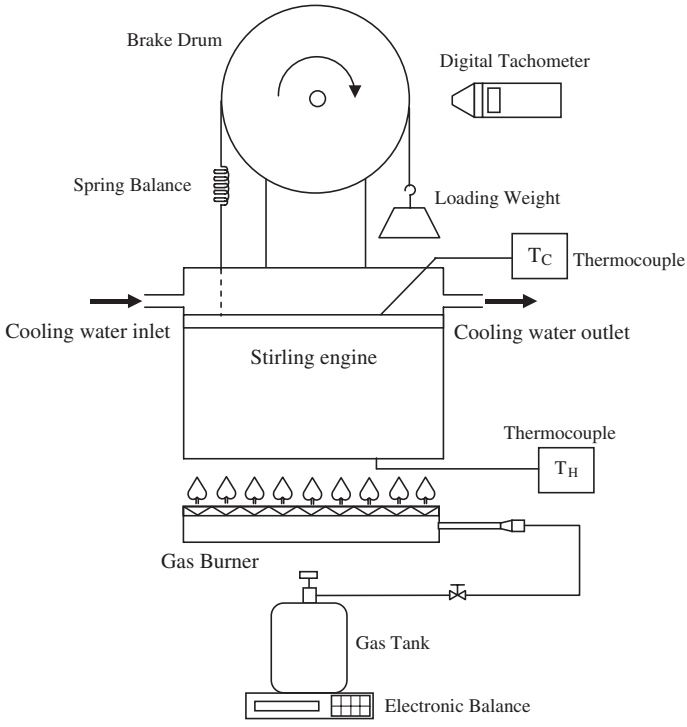

Fig. 3. Schematic diagram of the Stirling engine and testing facilities.

A domestic gas burner equipped with a LPG tank, a pressure regulator, and an adjustment valve is used to power the engine. An electronic balance and a stopwatch are used to measure the gas consumption. The accuracy of the gas mass measurement is ± 0.001 kg. The accuracy of the time measurement is ± 0.01 s. The higher and lower heating values of the gas used are 50 and 46 MJ/kg, respectively.

4. Experimental procedure

Before the engine is started, all thermocouples are connected to the data logger and computer. The cooling water system is connected to the engine cooling-pan. The cooling water flow rate is adjusted in order to keep the water level in the cooling-pan constant.

The domestic gas burner is placed underneath the displacer head. Then the gas tank is placed on the electronic balance and the initial gas mass is recorded.

Some lubricating oil is ejected into the power pistons, cylinders, and the displacer guide bushing. The gas burner is then fired and the gas flow rate is kept constant throughout the testing. The displacer head is heated up until it reaches the operating temperature. The engine is then started and run until the steady condition is reached.

The engine is loaded by adding a weight to the dynamometer. After that, the engine speed values, spring balance readings and all temperatures from the thermocouples are collected. Another loading weight is added to the dynamometer until the engine is stopped. Finally, the final gas mass and time taken in testing are recorded.

The testing can be repeated with another heat input by changing the gas flow rate. In this study, the engine test is performed at four values of constant burner heat input.

5. Results and discussions

Figs. 4–12 show the engine test results of the twin power piston engine. In these figures, the engine torque is calculated from:

$$T = (S - W)r \tag{1}$$

where S is the spring balance reading and W is loading weight, and r is brake drum radius. The actual shaft power can be calculated from:

$$P = 2\pi TN \tag{2}$$

where N is engine speed. E_{BT} is brake thermal efficiency calculated from:

$$E_{BT} = P/q_{in} \tag{3}$$

where q_{in} is the actual heat input to the engine. The actual heat input to the engine can be determined from:

$$q_{in} = E_H\, q_S \tag{4}$$

where E_H is heat source efficiency and q_S is total heat input from a heat source.

For a gas burner, the heat source (burner) efficiency can be calculated from [16] as follows:

$$E_H = \frac{m_w C_P (T_{w2} - T_{w1})}{m_f H} \tag{5}$$

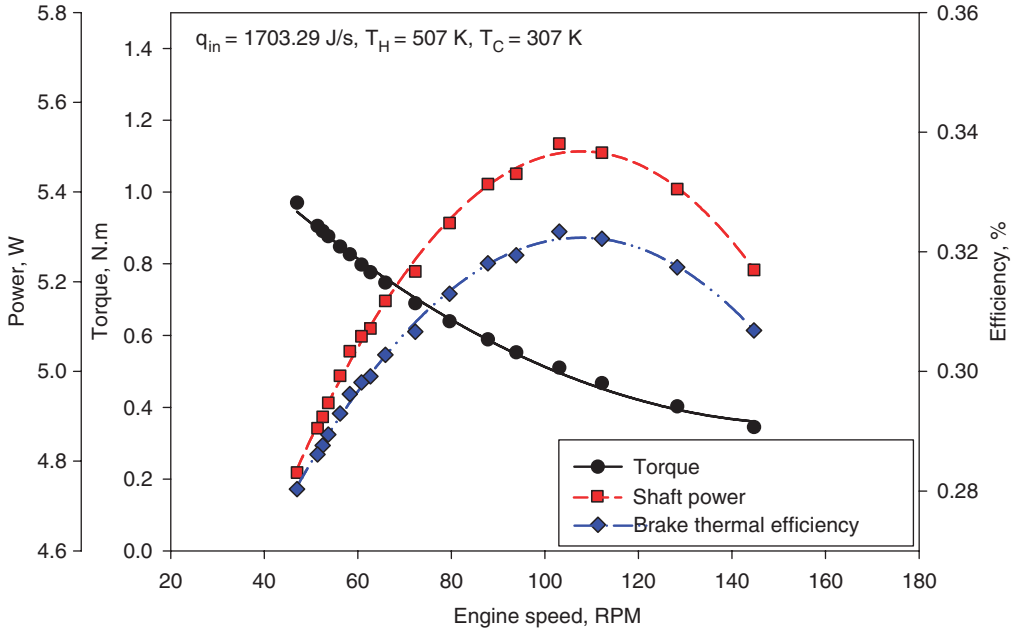

Fig. 4. Twin power piston engine performance at the actual heat input of 1703.29 J/s.

where m_w is the mass of water to absorb heat, C_P is the specific heat of water at constant pressure, T_{w1} and T_{w2} are, respectively, the initial water temperature and the maximum water temperature after the burner has been turned off, m_f is the mass of gas burned and H is the lower heating value of the gas.

The actual heat input to the engine q_{in}, at the heat input values from the heat source, q_S, of 5865, 6816, 7591, and 7880 J/s was experimentally determined by using water to absorb this heat. The actual heat input to the engine, the heat source efficiency and the absorber temperatures resulting from these simulated intensities are shown in Table 3.

Figs. 4–7 show the engine performance at 1703.29, 1996.18, 2256.26, and 2355.23 J/s actual heat input, respectively. These performance characteristic curves are quite similar to that of the piston-type internal combustion engine. The performance curves of this engine are described as follows:

In an engine test, after the load is gradually applied to the engine, the engine speed will gradually reduce until a certain applied load will stop the engine. The characteristics are represented by the curve of torque versus engine speed. In these figures, it can be noted that the engine torque decreases with increasing engine speed.

The variations of shaft power with engine speed are also shown in these figures. The shaft power increases with increasing engine speed until the maximum shaft power is reached and then decreases with increasing engine speed. The decreasing shaft power after the maximum point results from the friction that increases with increasing speed together with inadequate heat transfers at higher speed.

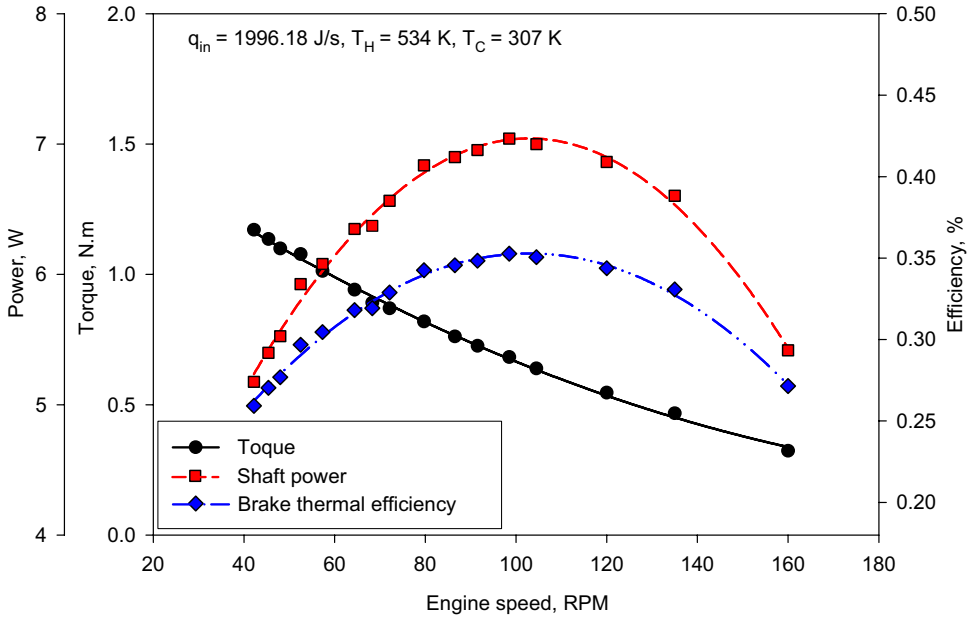

Fig. 5. Twin power piston engine performance at the actual heat input of 1996.18 J/s.

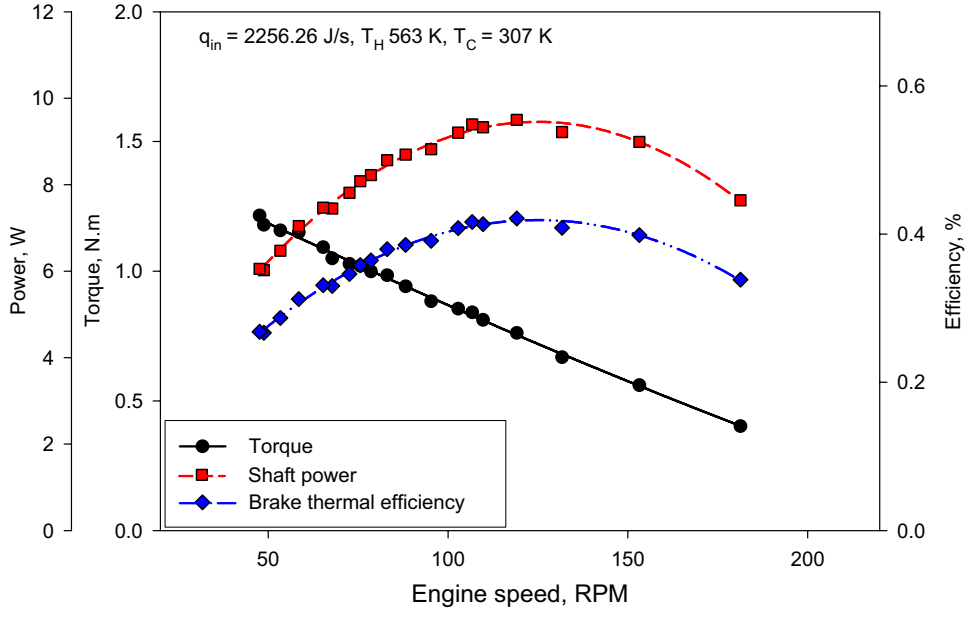

Fig. 6. Twin power piston engine performance at the actual heat input of 2256.26 J/s.

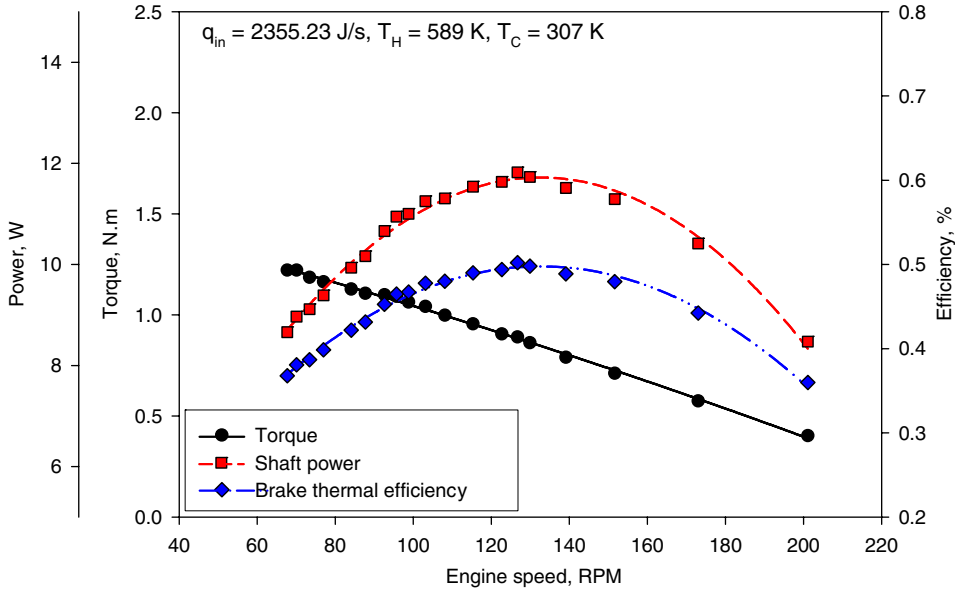

Fig. 7. Twin power piston engine performance at the actual heat input of 2355.23 J/s.

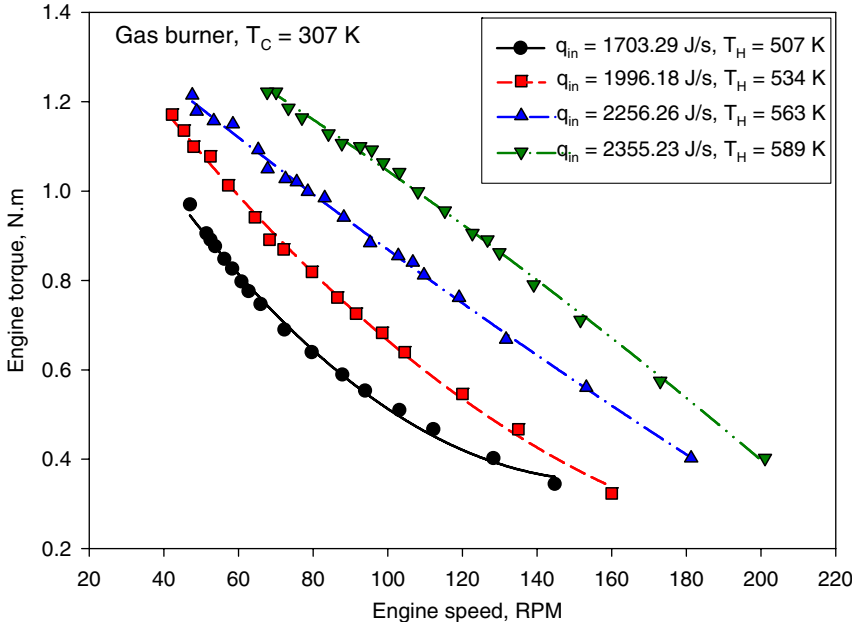

Fig. 8. Variations of twin power piston engine torque at various actual heat inputs.

Since brake thermal efficiency is the shaft power divided by a constant heat input, the curve of the brake thermal efficiency has the same trend as the shaft power. The very low-thermal efficiency may be caused by engine part machining problems encountered

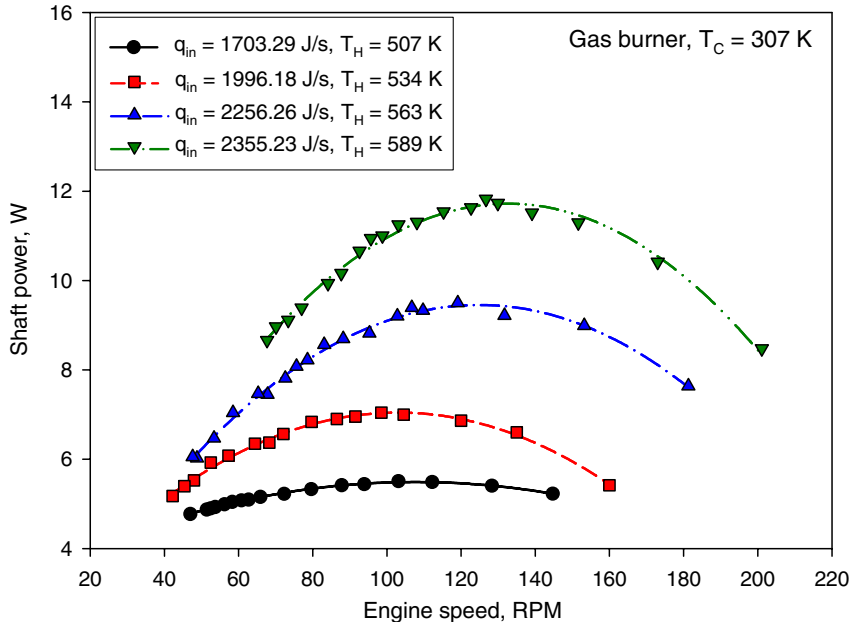

Fig. 9. Variations of twin power piston engine shaft power at various actual heat inputs.

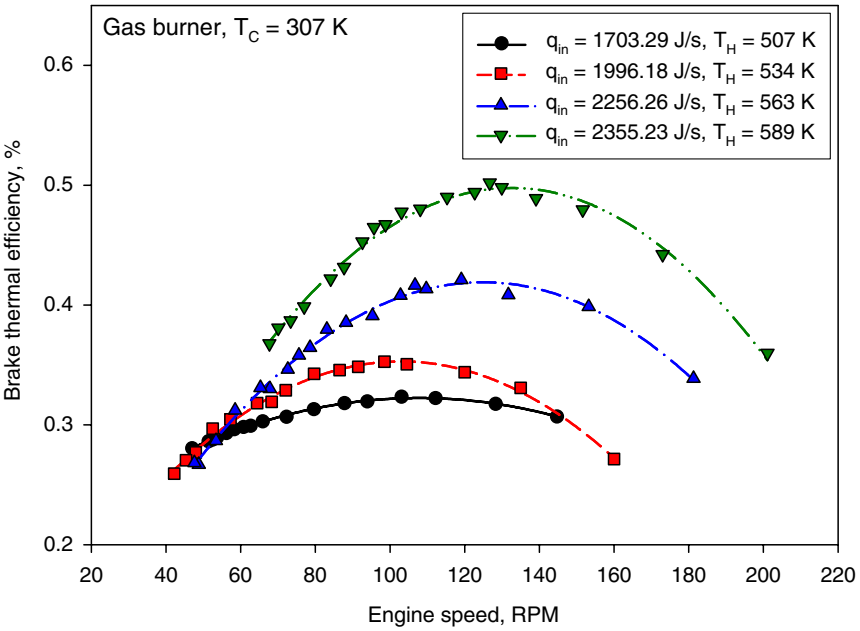

Fig. 10. Variations of twin power piston engine brake thermal efficiency at various actual heat inputs.

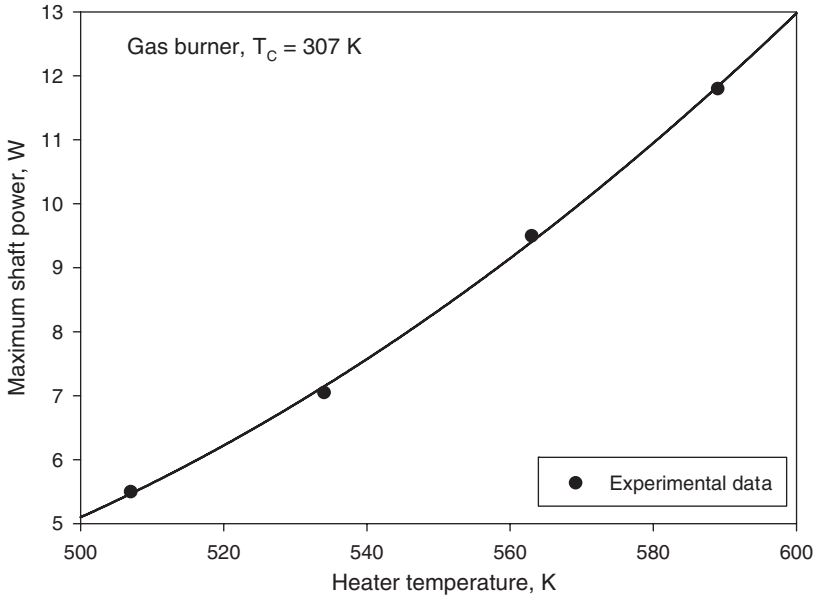

Fig. 11. Variations of twin power piston engine maximum shaft power with heater temperature.

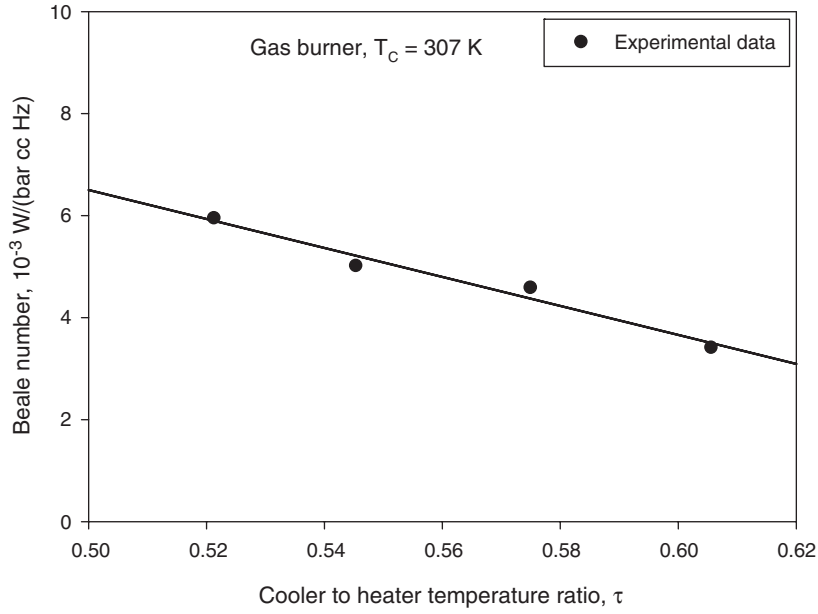

Fig. 12. Variations of twin power piston engine Beale number with temperature ratio.

during the manufacture of this engine. This causes the engine to have some misalignments and higher friction. Another cause is that the engine operates at relatively low temperature. The gas burner efficiency, distance from burner to displacer head, the displacer head thickness, and convection heat loss also affect the thermal efficiency.

Figs. 8–10 show the variations of the engine torque, shaft power, and brake thermal efficiency at various heat inputs with engine speed. As expected, the greater engine performance results from the higher heat input. An increase of the engine torque, shaft power and brake thermal efficiency is shown to also depend on the heater temperature. The value for maximum torque, shaft power and brake thermal efficiency are summarized in Table 3.

The maximum shaft power at various heat inputs is plotted against the heater temperature in Table 3. The plot is shown in Fig. 11. In this figure, the shaft power increases as a function of the heater temperature. Therefore, a greater maximum shaft power will be obtained from a higher heater temperature.

Table 3 also shows the Beale number obtained from this engine at various heat inputs. These Beale numbers are plotted versus the temperature ratio, $\tau = T_C/T_H$. The plot is shown in Fig. 12. The Beale number is calculated from the Beale formula [13,14]:

$$N_B = P/(p_m V_P f) \tag{6}$$

Table 3
Maximum engine performance and Beale number of twin power piston engine ($T_C = 307$ K)

q_S (J/s)	q_{in} (J/s)	E_H (%)	T_H (K)	T (N m)	P_{max} (W)	E_{BT} (%)	τ	N_B (W/bar cc Hz)
5865	1703.29	29.04	507	0.970 at 47.0 rpm	5.50 at 108 rpm	0.322 at 108 rpm	0.6055	3.4185×10^{-3}
6816	1996.18	29.29	534	1.171 at 42.2 rpm	7.05 at 103 rpm	0.354 at 103 rpm	0.5749	4.5946×10^{-3}
7591	2256.26	29.72	563	1.214 at 47.6 rpm	9.50 at 127 rpm	0.419 at 127 rpm	0.5435	5.0213×10^{-3}
7880	2355.23	29.89	589	1.222 at 67.7 rpm	11.8 at 133 rpm	0.494 at 133 rpm	0.5212	5.9556×10^{-3}

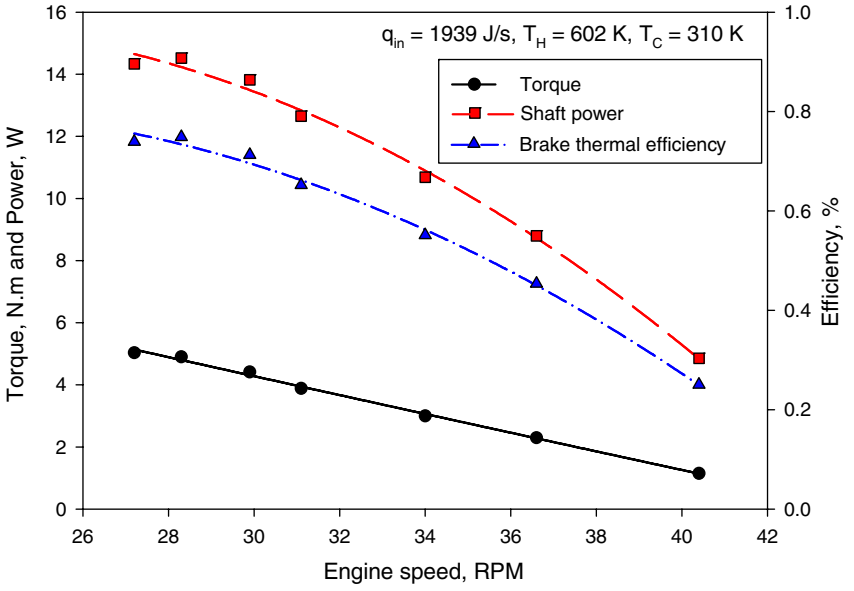

Fig. 13. Four power pistons engine performance at the actual heat input of 1939 J/s.

where p_m is engine mean pressure (bar), V_P is power-piston swept volume (cc), and f is engine frequency (Hz). For a non-pressurized engine, $p_m = 1$ bar is used in calculations, as described by Senft [2]. From this figure, it can be seen that the Beale number decreases with increasing temperature ratio. In other words, it can be said that the Beale number increases with increasing heater temperature.

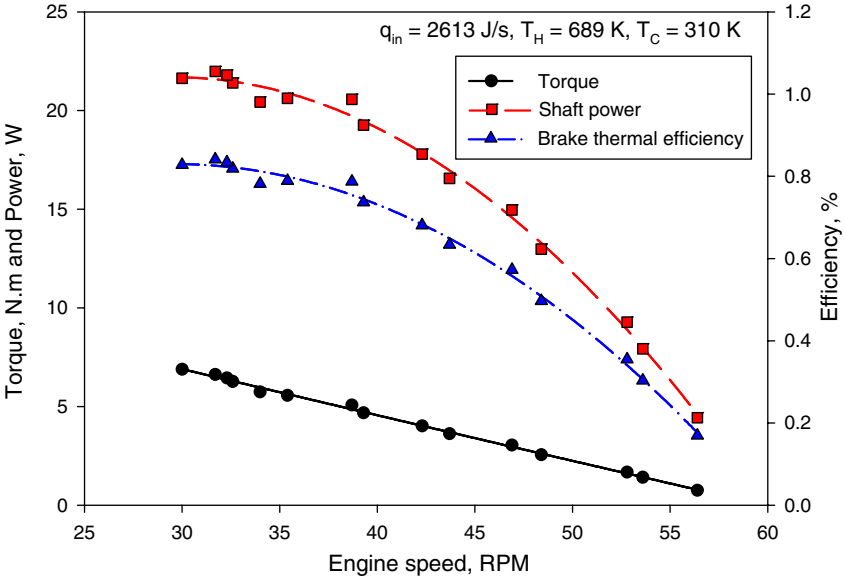

Fig. 14. Four power pistons engine performance at the actual heat input of 2613 J/s.

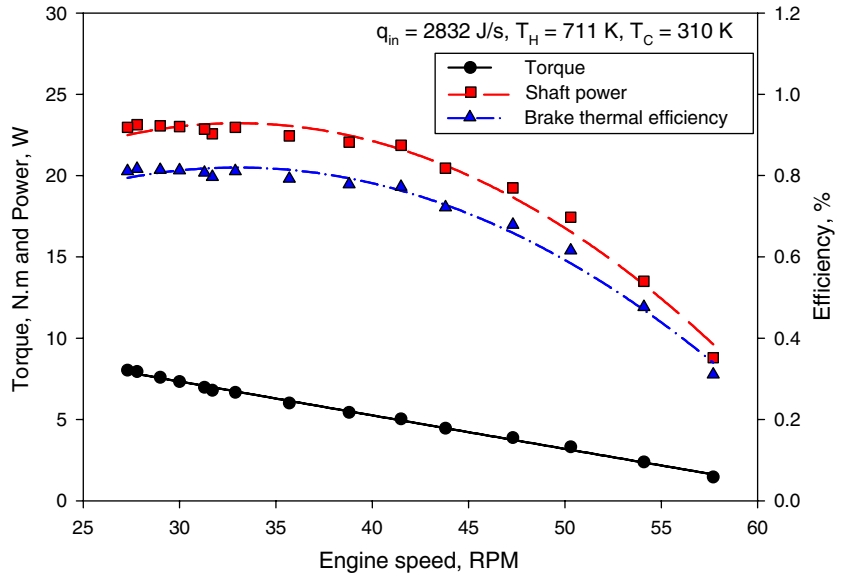

Fig. 15. Four power pistons engine performance at the actual heat input of 2832 J/s.

Test results of the four power pistons with the heat source, q_S, of 4112, 5666, 6189, 6778 and 9235 J/s are shown in Figs 13–22 and the maximum performances are summarized in Table 4. It can be noted that, these characteristic curves are similar to those of the twin power piston engine.

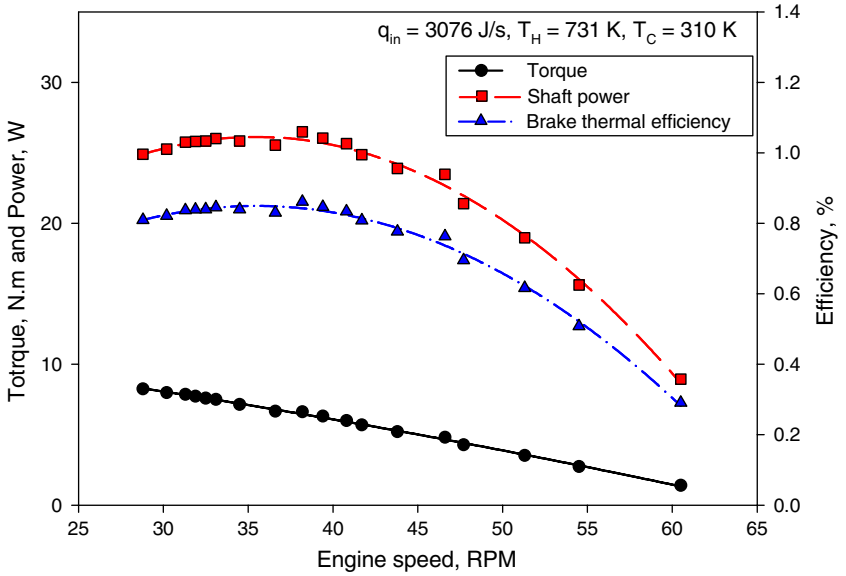

Fig. 16. Four power pistons engine performance at the actual heat input of 3076 J/s.

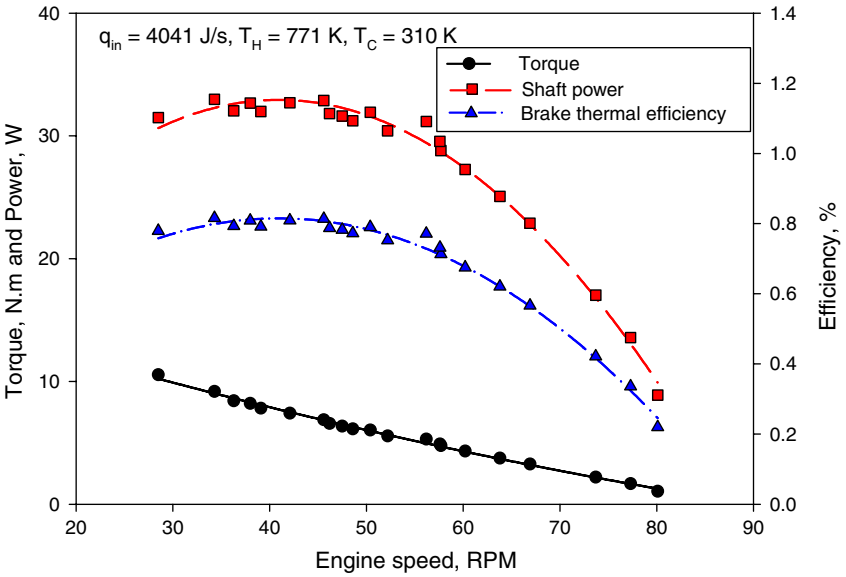

Fig. 17. Four power pistons engine performance at the actual heat input of 4041 J/s.

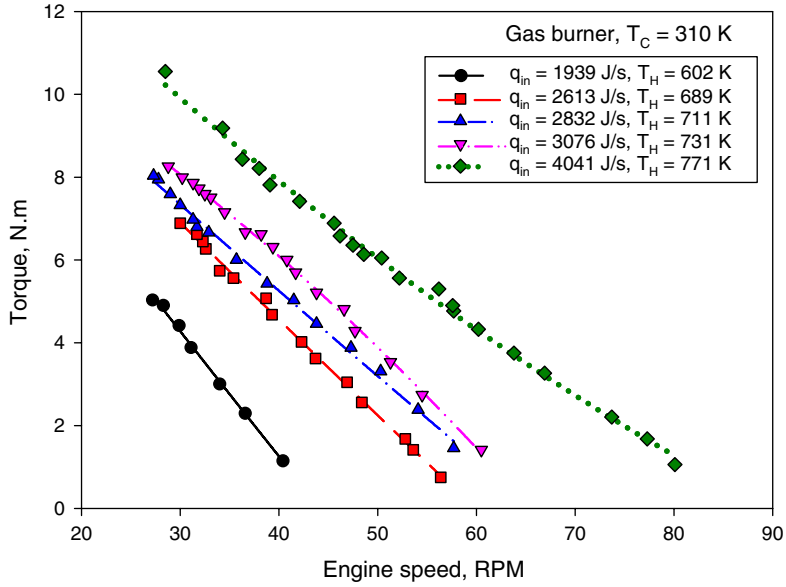

Fig. 18. Variations of four power pistons engine torque at various actual heat input.

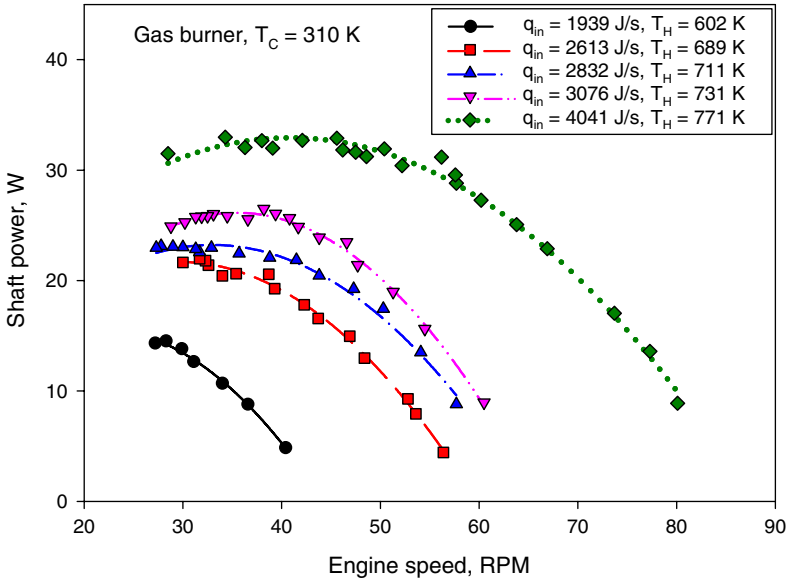

Fig. 19. Variations of four power pistons engine shaft power at various actual heat input.

6. Conclusions

In this experimental investigation, two kinematic, single-acting, twin power piston and four power pistons, gamma-configuration LTD Stirling engines were designed, constructed and tested with a domestic gas burner by using non-pressurized air as a working fluid.

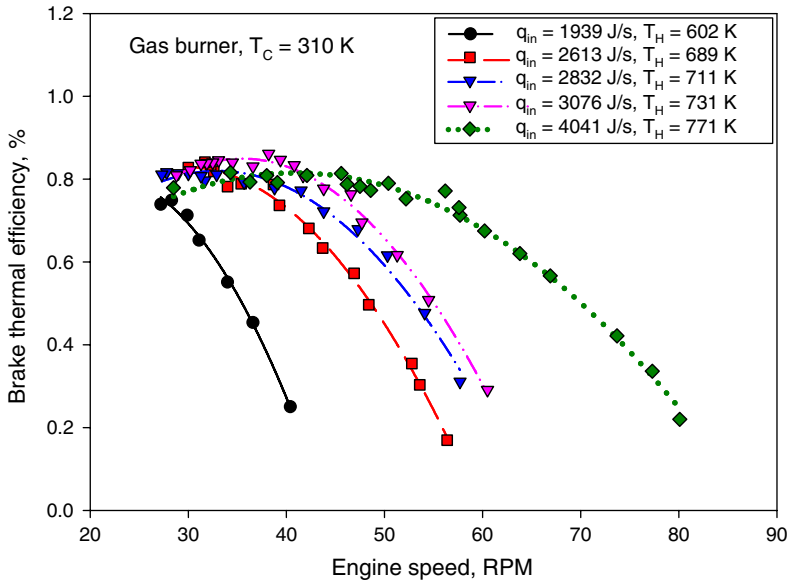

Fig. 20. Variations of four power pistons engine brake thermal efficiency at various actual heat input.

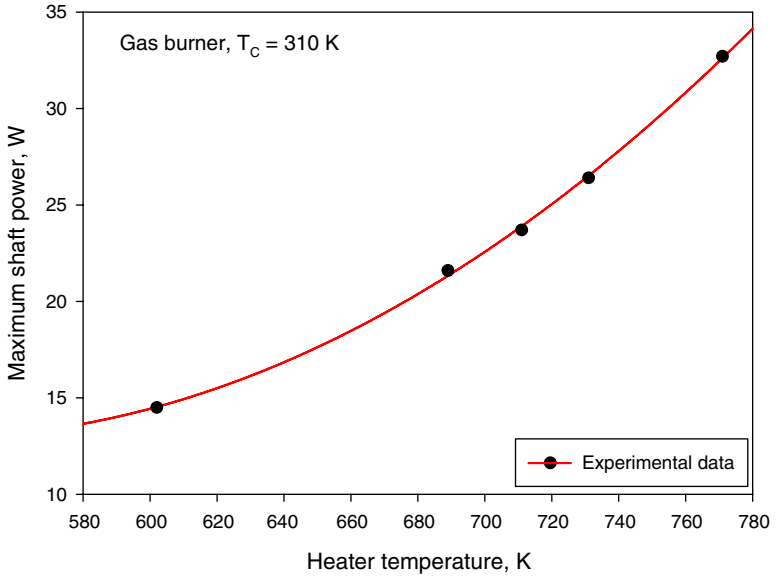

Fig. 21. Variations of four power pistons engine maximum shaft power with heater temperature.

The engine was tested with various constant heat input values. From this study, the following conclusions are drawn:

1. Results from this study indicate that the engine performance will increase with increasing heat input. The engine torque, shaft power, brake thermal efficiency, speed, and heater temperature also increase with increasing heat input.

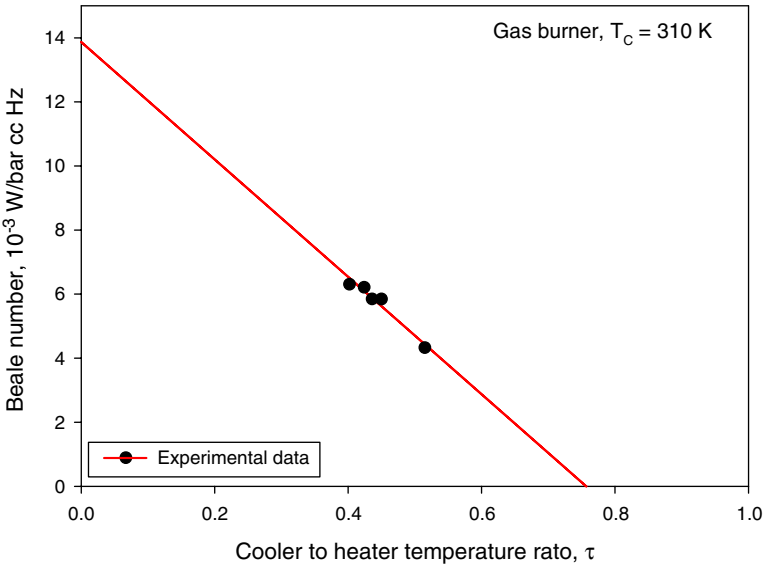

Fig. 22. Variations of four power pistons engine Beale number with temperature ratio.

Table 4
Maximum engine performance and Beale number of four power pistons engine ($T_C = 307$ K)

q_S (J/s)	q_{in} (J/s)	E_H (%)	T_H (K)	T (N m)	P_{max} (W)	E_{BT} (%)	τ	N_B (W/bar cc Hz)
4112	1939	47.15	602	5.03 at 27.2 rpm	14.5 at 27.2 rpm	0.748 at 27.2 rpm	0.510	4.3276×10^{-3}
5666	2613	46.12	689	6.89 at 30.0 rpm	21.6 at 30.0 rpm	0.827 at 30.0 rpm	0.446	5.8449×10^{-3}
6189	2832	45.78	711	8.03 at 27.3 rpm	23.7 at 32.9 rpm	0.837 at 32.9 rpm	0.432	5.8479×10^{-3}
6778	3076	45.39	731	8.26 at 28.8 rpm	26.4 at 35.4 rpm	0.858 at 35.4 rpm	0.420	6.2120×10^{-3}
9235	4041	43.76	771	10.55 at 28.5 rpm	32.7 at 42.1 rpm	0.809 at 42.1 rpm	0.398	6.3054×10^{-3}

2. At the maximum actual heat input of 2355.23 J/s, with a heater temperature of 589 K, the twin power piston engine produced a maximum torque of 1.222 N m at 67.7 rpm, a maximum shaft power of 11.8 W at 133 rpm, and a maximum brake thermal efficiency of 0.494% at 133 rpm, approximately.
3. At the maximum actual heat input of 4041 J/s, with the heater temperature of 771 K, the four power pistons engine produced a maximum torque of 10.55 N m at 28.5 rpm, a maximum shaft power of 32.7 W at 42.1 rpm, and a maximum brake thermal efficiency of 0.809% at 42.1 rpm, approximately.
4. In fact, it can be said that the maximum engine torque, shaft power, and brake thermal efficiency increase with increasing heater temperature.
5. The Beale number of this engine increases with decreasing temperature ratio or with increasing heater temperature.

The engine performance can be improved by increasing the precision of engine parts and the heat source efficiency. The engine performance should be increased if a better working

fluid e.g. helium or hydrogen is used instead of air and/or by operating the engine at some degree of pressurization.

Acknowledgments

The authors would like to express their appreciation to the Joint Graduate School of Energy and Environment (JGSEE) and the Thailand Research Fund (TRF) for providing financial support for this study.

References

[1] Rizzo JG. The Stirling engine manual. Somerset: Camden miniature steam services; 1997 p. 1, 43, 153, 155.
[2] Senft JR. Ringbom Stirling engines. New York: Oxford University Press; 1993 p. 3, 72, 88, 110, 113–37.
[3] Walpita SH. Development of the solar receiver for a small Stirling engine. Special study project report no. ET-83-1. Bangkok: Asian Institute of Technology; 1983. p. 3.
[4] West CD. A historical perspective on Stirling engine performance. Proceedings of the 23rd intersociety energy conversion engineering conference, Paper 889004. Denver: American Society of Mechanical Engineers; 1988.
[5] Van Arsdell BH. Stirling engines. In: Zumerchik J, editor. Macmillan encyclopedia of energy, vol. 3. Macmillan Reference USA; 2001. p. 1090–5.
[6] Kongtragool B, Wongwises S. A review of solar powered Stirling engines and low temperature differential Stirling engines. Renewable Sustainable Energy Rev 2003;7:131–54.
[7] Haneman D. Theory and principles of low-temperature hot air engines fuelled by solar energy. Report Prepared for U.S. Atomic Energy Commission Contract W-7405-Eng-48; 1975.
[8] Spencer LC. A comprehensive review of small solar-powered heat engines: Part III. Research since 1950-"unconventional" engines up to 100 kW. Sol Energy 1989;43:211–25.
[9] White EW. Solar heat engines, U.S. Patent; 1983. p. 4, 414, 814.
[10] O'Hare LR. Convection powered solar engine, U.S. Patent; 1984. p. 4, 453, 382.
[11] Senft JR. An ultra-low temperature differential Stirling engine. Proceeding of the fifth international stirling engine conference, Paper ISEC 91032, Dubrovnik, May 1991.
[12] Iwamoto I, Toda F, Hirata K, Takeuchi M, Yamamoto T. Comparison of low-and high-temperature differential Stirling engines. Proceedings of eighth International Stirling engine conference, 1997. 29–38.
[13] Kongtragool B, Wongwises S. Theoretical investigation on Beale number for low-temperature differential Stirling engines. Proceedings of the second international conference on heat transfer, fluid mechanics, and thermodynamics 2003 (Paper no. KB2, Victoria Falls, Zambia).
[14] Kongtragool B, Wongwises S. Investigation on power output of the gamma-configuration low temperature differential Stirling engines. Renewable Energy 2005;30:465–76.
[15] Kongtragool B, Wongwises S. Optimum absorber temperature of a once-reflecting full conical concentrator of a low-temperature differential Stirling engine. Renewable Energy 2006;31:345–59.
[16] European Standard, Domestic cooking appliances burning gas, EN 30 2nd ed., January 1979.